JOURNAL OF MATERIALS SCIENCE 26 (1991) 1565–1576

Alternating-current electrical properties of random metal–insulator composites

IN-GANN CHEN*, W. B. JOHNSON‡
Department of Materials Science, Ohio State University, 116 West 19th Avenue, Columbus, Ohio 43210, USA

The complex a.c. impedance of three different random metal–insulator composites near their percolation threshold has been studied. These three metal–insulator systems include different shapes of nickel particles (filamentary and nodular shapes) in a matrix of polypropylene and silver particles in the matrix of potassium chloride. By using different metal–insulator structures and phases it is possible to elucidate the effect of different metal particle shapes and types of insulator phase on the electrical properties of these composites near their percolation threshold. Electrical properties, including d.c. conductivity, a.c. conductance, capacitance and dielectric loss tangent, of these metal–insulator composites as a function of metal volume fraction and frequency (5 Hz to 13 MHz) are presented. The results are correlated with structural characterization of these composites and are used to examine the applicability of different electrical transport models on these composite materials. The effect of different metal particle shapes on the percolation threshold and the power-law dependent percolation phenomenon is also discussed.

1. Introduction

The electrical properties of random metal–insulator composites, which are composed of metal particles or conductive fibres randomly dispersed in an insulating matrix, have been a subject of interest to both solid-state physicists for theoretical reasons and polymer engineers for practical applications. These composites, which have a higher electrical conductivity than most polymers, are widely used in electromagnetic shielding for electrical devices as well as in eliminating electrostatic charge build-up for preventing damage to electronic components [1, 2]. More recently, the electrical properties of newly discovered high-T_c superconducting oxide–metal random composites were also studied for both their practical and theoretical significance [3, 4]. It is well known that electrical conductivity changes by orders of magnitude from an insulator to a conductor in a narrow range of metal volume fractions. The observation of the transition behaviour in such metal–insulator composites is often called a percolation phenomenon, and the critical point is known as the percolation threshold (P_c). Broadbent and Hammersley [5] introduced a physical model, i.e. the percolation model, to describe this transition behaviour. Based on the percolation model, the relationships between the electrical properties, such as conductance (G) and dielectric constant (K), and the metal volume fraction (P) near the percolation threshold generally obey power-law dependencies on the distance-from-threshold ($P - P_c$) as

$$G(P) \propto (P - P_c)^t \qquad (1)$$

$$K(P) \propto (P_c - P)^{-s} \qquad (2)$$

where t and s are critical exponents associated with G and K [6, 7]. Moreover, based on the computer simulation on random conductor–insulator networks, the critical exponents discussed above are proposed to be insensitive to the details of conductive cluster geometry with the same dimensionality [8, 9]. In other words, universal critical exponents t and s were proposed based on computer simulations. Here, experimental study of the effect of geometric differences in metal particles has been conducted to examine the influence of metal phase geometrical shape on the electrical properties of the random composites.

The effects of small a.c. signals of different frequencies on the a.c. electrical properties of three-dimensional random metal–insulator composites have also been reported [10–12]. For specimens close to the percolation threshold, it is observed that both a.c. conductance and a.c. dielectric constant follow a power-law relationship with frequency:

$$G(\omega, P_c) \propto \omega^x \qquad (3)$$

$$K(\omega, P_c) \propto \omega^{-y} \qquad (4)$$

$$x + y \simeq 1 \qquad (5)$$

where ω is the frequency, and x and y are exponents associated with the frequency-dependent G and K.

An experimental study by Hamon [13] on the dielectric loss factor of copper phthalocyanine powder in the matrix of paraffin wax shows a strong frequency dependence as the copper phthalocyanine concentra-

---

**Present address*: Texas Center for Superconductivity, University of Houston, Houston, TX 77204-5506, USA.
‡Present address: Lanxide Corp., Tralee Industrial Park, Newark, DE 19714-6077, USA.

0022–2461/91 $03.00 + .12

tion increases. This frequency-dependent phenomenon has been attributed to the existence of conducting paths through copper phthalocyanine particles. In this paper, the dielectric loss tangent of these metal–insulator random composites near the percolation threshold has been studied and a power-law behaviour is described as the metal volume fraction approaches the percolation threshold.

The general a.c. electrical transport problems as well as the effect of metal particle shape and insulating phase in this composite system on these properties will also be examined. Three systems of random metal–insulator composites near their metal-to-insulator transition, i.e. percolation threshold, region have been studied. These three systems include filamentary and nodular shape nickel particles in the matrix of polypropylene, abbreviated as (Ni/F–PP) and (Ni/N–PP) respectively, and silver particles in the matrix of potassium chloride (Ag–KCl). These composites have all been prepared by mechanically mixing metal and insulator particles in predetermined volume fractions. Filamentary shape nickel particles show a spiky surface geometry and tend to form long chain-like agglomerates, while nodular-shaped nickel particles have much less of a tendency to form clusters. This geometric difference in metal particles has been used to study the influence of metal phase geometrical shape on the electrical properties. The Ag–KCl system is a metal–ionic salt composite, and the Ni–PP system is a metal–polymer composite. The effect of matrix phase on the electrical properties has been studied.

D.c. conductivity as well as the a.c. electrical properties including, a.c. conductivity, a.c. dielectric constant and a.c. dielectric loss tangent have been investigated as a function of metal volume fraction. The complex a.c. impedance between 5 Hz and 13 MHz, which covers the range of long radio-wave frequency and is well below that accessible to infrared spectrometers, should provide a comprehensive picture of the electromagnetic properties of the composites near percolation. The applicability of percolation theory to the results will also be discussed.

2. Experimental procedure

2.1. Sample preparations

For Ni/F–PP and Ni/N–PP specimens, pre-weighed metal and insulator powders in appropriate ratios were thoroughly mixed using a vortex mixer and metal ball milling. X-ray energy-dispersive spectrum (EDS) analyses of the mixed powders were performed and showed no detectable level of contamination from metal ball-milling. The mixed powder was then pressed into a pellet using a hydrostatic press with a maximum pressure of 900 MPa. During the pressing process, the die was slowly heated from 95 to 100 °C, which is above the heat deflection temperature of polypropylene (PP). The filamentary-shaped nickel (Ni/F) particles with a spiky surface (Fig. 1a) were formed into chain-like structures resembling strings of small nickel beads with an aspect ratio of about 5 to 10. Both PP and metal particles showed a log-normal distribution [14]. The nickel beads have an average bead size of 1.2 μm while the nodular shaped nickel particles have a rough surface with an average particle size of 9.2 μm. The PP particles have a rough surface and an irregular shape with an average particle size about 1.6 μm. Density measurements of Ni/F–PP and Ni/N–PP specimens were performed using Archimedes' method. No, or very low, porosity in the samples was observed after compaction.

The Ag–KCl specimens were prepared previously [7] using several pressing/grinding cycles of silver (average particle size 20 nm) and KCl powder. All three types of composite specimen were coated with either gold (by sputtering) or silver (with silver paste) to ensure good electrical contact on the surface of the specimen.

2.2. Electrical measurements

The d.c. resistance was obtained by calculating the slope of the d.c. I–V curve, measured using an HP4140b pA meter/d.c. voltage source instrument. All the resistance data shown in this report have a correlation coefficient of 0.90 and above for the slope calculation from the I–V curve. The a.c. impedance, dielectric constant (K) and dielectric loss tangent ($\tan\alpha$) measurements were made using the two-terminal pair technique with the length of the leads between electrode and apparatus as short as possible to minimize the effect of lead impedance. The data were also corrected for possible effects of lead impedance by subtracting the impedance measurement from an empty (shorted) cell. All the a.c. impedance measurements were made using an HP 4192-A low-frequency impedance analyser in the frequency range from 5 Hz to 13 MHz with 20 points per decade. Both K and $\tan\alpha$ are measured by using the HP 4192-A at the frequency of 100 kHz. Measured data were recorded using an IBM PC through a Tecmar PC-Mate IEEE-488 interfacing system. In all the a.c. impedance measurements, the oscillation level of the small a.c. signal applied was 10 mV and the reading for each frequency is the average value of five consecutive measurements.

3. Results and discussion

3.1. Effect of metal volume fraction on electrical properties

D.c. resistivity measurements of all three random composite system specimens are shown in Fig. 2. Some of the samples have resistivities that exceed the limitation of the instrument ($> 1.0 \times 10^{14}\,\Omega$) and are shown with an arrow in Fig. 2. The value of P_c can be estimated visually from Fig. 2 by the range of metal-to-insulator transition marked by the arrows, i.e. P_c ranges from about 0.26 to 0.29 (0.275 ± 0.015) for Ni/N–PP, 0.07 to 0.09 (0.08 ± 0.01) for Ni/F–PP, and 0.21 for Ag–KCl composites.

The theoretical prediction of the percolation threshold for a three-dimensional random system was first found through numerical simulation by Scher and Zallen to be about 0.16 [15]. This P_c value is invariant for systems with various lattice structures which are occupied randomly by proportional amounts of

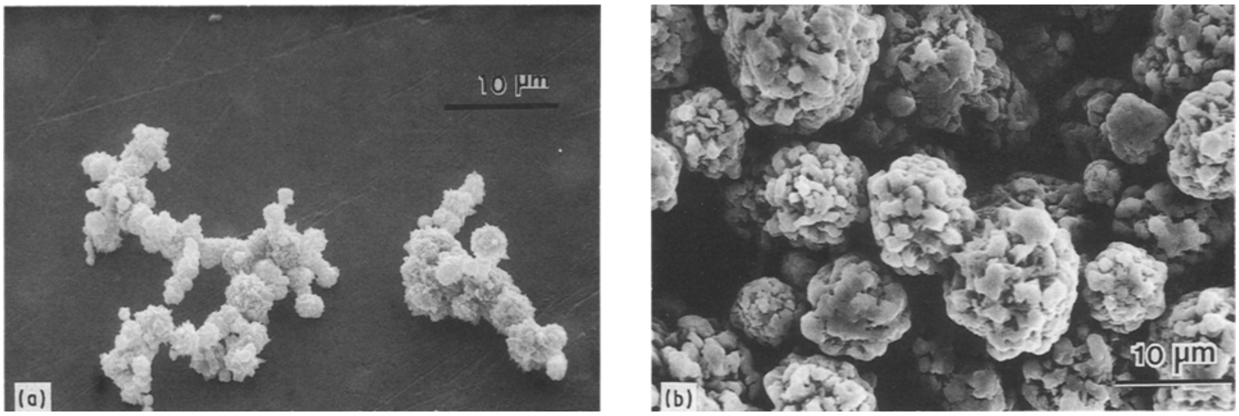

Figure 1 Scanning electron microscopy images of (a) filamentary shape, spiky surface nickel particles and (b) nodular shape nickel particles.

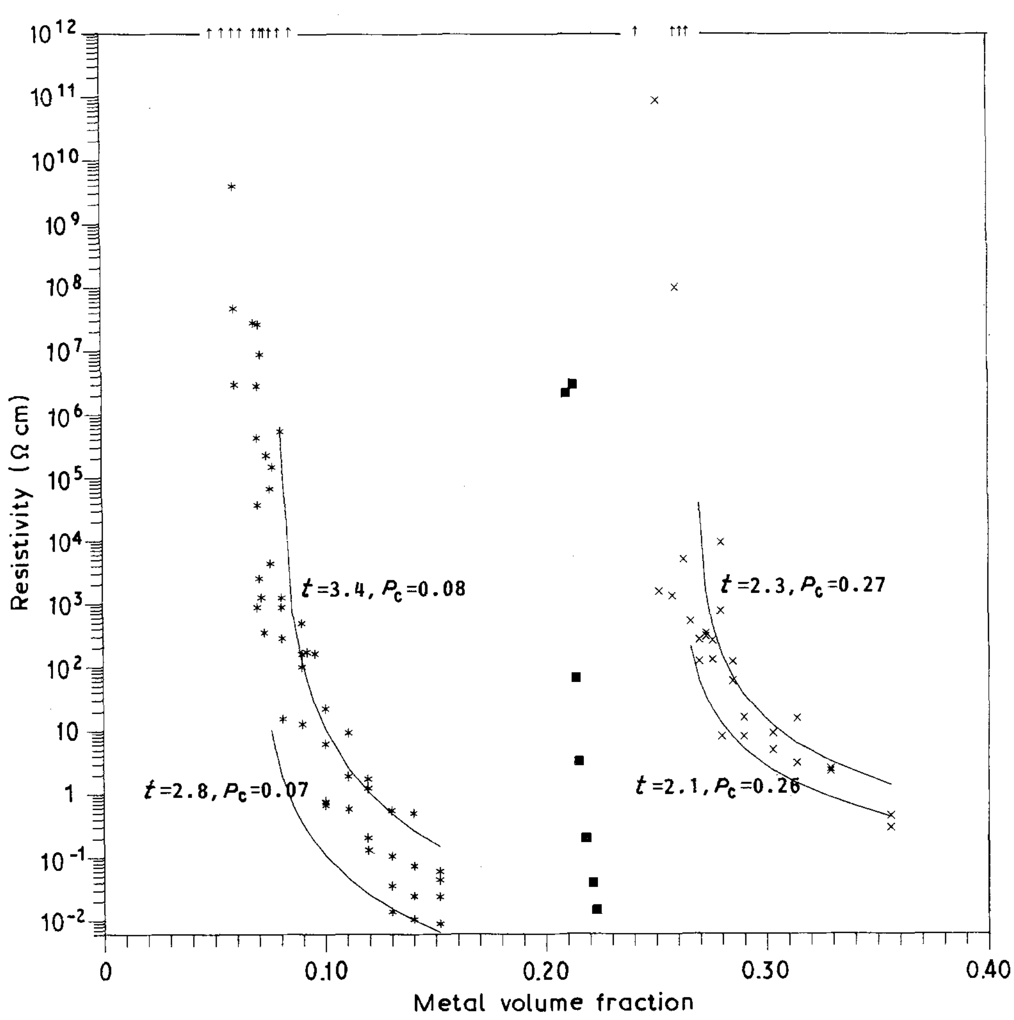

Figure 2 D.c. resistivity measurements of all three systems of samples as a function of metal volume fraction. The arrows indicate samples with resistivity too high to measure accurately with the instrumentation available. Solid lines represent the normalized power-law relationship $R \propto [(P - P_c)/P_c]^{-t}$ between resistivity and metal volume fraction corresponding to Equation 1. (*) Ni/F–PP, (×) Ni/N–PP, (■) Ag–Cl.

conductive or insulating particles [9]. However, the lattice structures used in these simulations presumed that metal and insulating particles are spherical with the same and constant sizes, which is rarely seen in practical systems. Recently, these constraints have been lifted and simulations show different P_c values for different particle shapes and sizes [16]. Experimental results show that the percolation threshold varies with different metal–insulator systems and depends primarily on the metal particle shape, size distribution and extent of segregation, as well as the processing method of the composite [2, 17]. An increase in the aspect ratio (longest dimension to lowest dimension) of the conductive particle will shift the percolation threshold to lower concentration [1, 18, 19], because the higher the aspect ratio, the higher the

TABLE I Summary of the power-law relationships and their critical exponent values obtained in this study and previously

Power-law relationship	Critical exponent	This study			Literature		
		Ag–KCl	Ni/F–PP	Ni/N–PP	Chain-like or fibre	Spherical	Computer simulation
$G \propto \left(\frac{P-P_c}{P_c}\right)^t$ or $R \propto \left(\frac{P-P_c}{P_c}\right)^{-t}$	t		3.1 ± 0.3	2.2 ± 0.1	3.0 ± 0.6* 1.9 ± 0.2†	1.85 ± 0.25‡ 2.15 ± 0.25§ 2.30 ± 0.40a 1.90 ± 0.20b	1.85 ± 0.15¶
$C \propto \left(\frac{P_c-P}{P_c}\right)^s$	s		0.55 ± 0.10	0.62 ± 0.10		0.68 ± 0.05‡ 0.73 ± 0.07c	0.81 ± 0.08¶
$\tan\alpha \propto \left(\frac{P_c-P}{P_c}\right)^{-r}$	r		2.0 ± 0.2	1.1 ± 0.2			
$G \propto \omega^x$	x	0.77 ± 0.01	0.88 ± 0.01	0.81 ± 0.01		0.86 ± 0.08‡	
$C \propto \omega^{-y}$	y	0.22 ± 0.01	0.14 ± 0.01	0.13 ± 0.04		0.12 ± 0.04‡	
$\tan\alpha \propto \omega^{-z}$	z		0.71 ± 0.01	0.86 ± 0.01			
Percolation threshold	P_c	0.21 ± 0.01	0.08 ± 0.01	0.275 ± 0.015			

*Short carbon fibre in epoxy resin [26].
†Chain-like carbon powder in PVC, $P_c = 0.071 \pm 0.002$ [18].
‡Amorphous carbon in Teflon, $P_c = 0.290 \pm 0.005$ [12].
§Silver in copper oxide, $P_c = 0.062 \pm 0.01$ [25].
¶A review of computer simulation theoretical studies [24].
aCarbon in wax, $P_c = 0.108 \pm 0.001$ [36].
bTungsten in Al_2O_3, $P_c = 0.47 \pm 0.05$ [6].
cSilver in KCl, $P_c = 0.21 \pm 0.01$ [7].

probability of contact to other particles at a given metal volume fraction. Although Bigg [19] has proposed a power-law dependence between the conductive particle aspect ratio and the percolation threshold, the exact relationship has not been verified. Extensive studies of the dependence of the percolation threshold on the effect of fibre-orientation distribution, i.e. macroscopical anisotropy, as well as on fibre-length distributions in two- and three-dimensional systems have been investigated by Balberg and Binenbaum [20, 21] using a computer simulation technique.

Table I lists the results obtained in this investigation and previous comparable systems from literature. The P_c of the Ni/F–PP system is much lower than that of the Ni/N–PP system because of the larger aspect ratio of the Ni/F particles. The P_c of the Ni/N–PP system is in good agreement with the experimental result of 0.290 ± 0.005 for an amorphous carbon–Teflon composite [12]. On the other hand, the Ni/F–PP system is close to the value of 0.071 ± 0.002 for a chain-like carbon–PVC system [18]. These experimental P_c values deviate as expected from the value of 0.16 proposed by Scher and Zallen [15]. It has also been reported [22, 23] in several systems that a percolation threshold was not observed up to 0.45 volume fraction of conducting phase. One study used silver coated glass spheres in a matrix of polyester [22] while the other used various metal particles in a matrix of epoxy resin [23]. These spheres were mixed in polyester or epoxy resin with hardener followed by thermosetting into solid. In both these studies conducting particles appear to be separated from one another by a thin layer of plastic, presumably from the wetting between the resin and the surface of the conducting sphere [22, 23]. In this study, the composite samples were formed by pressing the metal–thermoplastic powder mixtures (Ni/F–PP and Ni/N–PP) so that wetting of the plastic on the metal particles is unlikely, leading to a lower percolation threshold. Clearly, though, the processing method is critically important to the electrical properties in general, and the location of the percolation threshold in particular in random metal–insulator composites.

Based on the percolation model, the relationships between the d.c. resistivity and the metal volume fraction (P) near the percolation threshold generally obey power-law dependences on the distance-from-threshold ($P - P_c$) as shown in Equation 1. To determine the critical exponent t for the d.c. resistivity, the resistivity was plotted against reduced metal volume fraction $(P - P_c)/P_c$ (Fig. 2). Using the best initial estimate of P_c described previously, the value of t was calculated. P_c was then adjusted and t recalculated. This iteration approach was repeated until the best fit to the data was obtained. For Ni/F–PP samples, t falls between 2.8 and 3.4 with $P_c = 0.08 \pm 0.01$. This result shows that a chain-like metal–insulator (Ni/F–PP) three-dimensional composite follows the percolation power-law behaviour which is generally observed in a system with spherical particles. A similar approach for the Ni/N–PP system gave t between 2.1 and 2.3 with $P_c = 0.265 \pm 0.005$. Data for the Ag–KCl system are not included for the fitting due to the limited number of specimens and the narrow compositional region of silver metal volume fraction.

The t values of Ni/N–PP and Ni/F–PP systems obtained in this investigation and previous comparable systems from the literature are listed in Table I. It has been generally accepted that the critical exponent t is insensitive to the lattice structures used in computer simulation experiments [8, 9]. As described previously, a lattice structure presumes a spherical shape and unique size. The Ni/N–PP system, which contains spherical conductive particles dispersed in an insulating matrix, shows t equal to 2.2 ± 0.1, which is in relatively good agreement with the computer simulated result of 1.85 ± 0.15 for a three-dimensional system [24] and the previous experimental results of 2.15 ± 0.25 [25] and 1.85 ± 0.25 [12]. For the Ni/F–PP system, on the other hand, t is equal to 3.1 $\pm$ 0.3 which is a higher t value than that predicted for three-dimensional systems with spherical conductive particles. Experimental work on such systems with non-spherically shaped conducting particles show $t = 1.9 \pm 0.2$ for a chain-like carbon–PVC composite [18] and $t = 3.0 \pm 0.6$ for a carbon fibre–epoxy composite [26]. The result of this study of the Ni/F–PP system shows a value of 3.1 ± 0.3 which is in close agreement with the carbon fibre–epoxy system. The large differences in exponents t for nickel particles of different shapes suggest that, instead of a universal exponent as suggested by computer simulation, the shape and size distribution of the conducting particle play an important role in the percolating power-law behaviour.

An additional feature in which the metal phase morphology plays a role is evident in Fig. 2. For the Ni/N–PP system only two data points show a resistivity which falls in the range between 10^4 and 10^{11} (Ω m), but there are more than ten readings for Ni/F–PP samples in the same resistivity range. One possible reason is that the metal particle size is much larger for Ni/N (mean diameter 9.2 μm) than Ni/F (mean diameter 1.2 μm). Thus, a single metal percolating cluster of the Ni/N–PP composite will allow much more current than that of the Ni/F–PP composite. Furthermore, the spiky structure of Ni/F particles (Fig. 1b) may even reduce the contact area in Ni/F clusters. In other words, a few percolating clusters near P_c allow a much more significant increase in conductance for Ni/N–PP composite than for Ni/F–PP composites.

For the resistivity measurements of both Ni/N–PP and Ni/F–PP systems shown in Fig. 2, an increased scatter in the data which is well above that expected from random sampling error is observed as the metal volume fraction approaches the percolation threshold P_c. The increased scatter in the data probably arises because in the region near the percolation threshold the number of percolation clusters, i.e. clusters that connect two sides of the specimen, plays an important role in the conductivity of the bulk composite. The probability of creating a percolation cluster rises sharply from zero and approaches unity at P_c due to the rapid increase in linkage between finite-size clusters and the percolation cluster [9, 27]. Since the creation of percolation clusters is a statistical phenomena, there is a given uncertainty associated with their creation. The wider the variation of particle size distribution and inhomogeneity, the larger the variation in the average number of particle contacts. Thus, a large uncertainty in the estimation of P_c will occur. Physically, a wider range of resistivity will be shown as the metal volume fraction approaches the percolation threshold. The average sample size of this study ranges from 50 to 100 mm^3, which contains about 10^8 to 10^{10} particles (including both nickel and PP) initially. This number is much larger than the capacity of regular computer simulation experiments. Though no such effect on conductivity near percolation has been predicted theoretically, an estimation of the effect of sample size on conductance fluctuation has been performed [28]. These results show that for the sample sizes used in this study, only a very small scatter would be expected [14].

3.2. A.c. measurements

The dielectric constant K as a function of metal volume fraction was measured at 100 kHz by an HP impedance analyser and the results are shown on a semi-log scale in Fig. 3 for all three metal–insulator systems studied. A divergent behaviour is observed as the metal volume fraction approaches the percolation threshold. Using an approach similar to that used to calculate the value of the critical exponent t, a value of the critical exponent s of Equation 2 was calculated for each system. Solid lines in Fig. 3 show the power-law relationships of the dielectric constant against reduced volume fraction for Ni/F–PP and Ni/N–PP systems. Data for the Ag–KCl system were not fitted because of the limited number of specimens and the narrow compositional region of silver metal volume fraction. These results show a power-law type dependence as predicted by the percolation theory with the critical exponent $s = 0.62 \pm 0.12$ for Ni/N–PP and $s = 0.55 \pm 0.10$ for Ni/F–PP systems. The constants s for both Ni/N–PP and Ni/F–PP systems show reasonable agreement with the value generated by computer simulation (0.81 ± 0.08 [24]) and by experiments (0.73 ± 0.07 [17] and 0.68 ± 0.05 [12]) for three-dimensional random metal–insulator composites with spherically shaped metal particles. The value of s, unlike the value of t, which is more dependent on the insulating matrix phase, depends weakly if at all on the metal particle morphology.

Divergent behaviour near P_c is also observed for the dielectric loss tangent tanα, as shown in Fig. 4 for each of the metal–insulator systems studied. A power-law relationship similar to Equation 2 is proposed to describe this phenomenon as

$$\tan\alpha \propto \left(\frac{P_c - P}{P_c}\right)^{-r} \qquad (6)$$

where r is the critical exponent associated with tanα. Solid lines in Fig. 4 show a relatively good agreement between the proposed power-law behaviour of Equation 6 and experimental results. The value of the critical exponent r was found to be equal to 2.0 ± 0.2

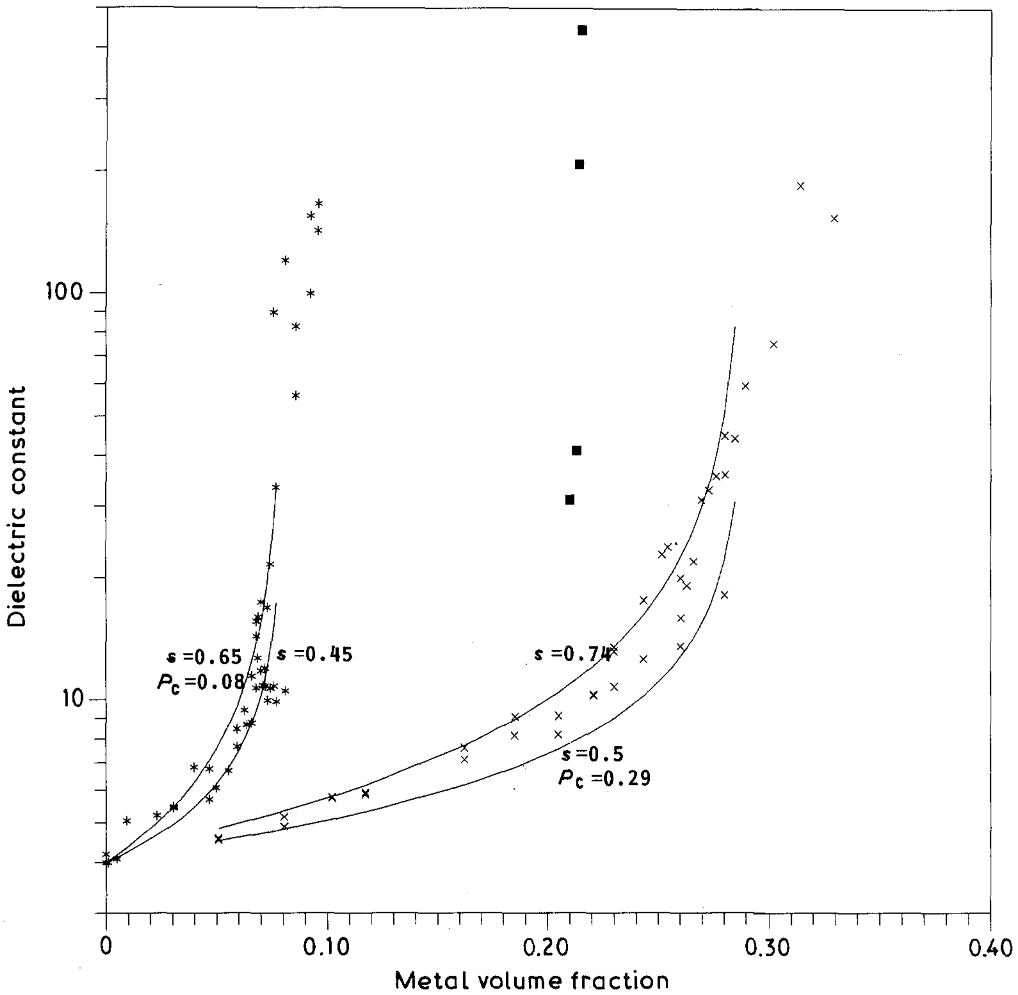

Figure 3 The dielectric constant K as a function of reduced metal volume fraction plotted using a semi-log scale. The solid lines show $K \propto [(P_c - P)/P_c]^{-s}$ (Equation 2) with $P_c = 0.08$ and $s = 0.55 \pm 0.10$ for the Ni/F–PP system and with $P_c = 0.29$ and $s = 0.62 \pm 0.12$ for the Ni/N–PP system. (∗) Ni/F–PP, (×) Ni/N–PP, (■) Ag–Cl.

for the Ni/F–PP and 1.1 ± 0.2 for the Ni/N–PP composite systems. No report on the dielectric loss tangent of random metal–insulator systems has been found to compare with previous results. The power-law behaviour holds for both dielectric constant and loss tangent over a wide range of metal volume fractions (0 to P_c for this study).

Assuming that the dielectric loss is caused only by d.c. conductivity, the dielectric loss tangent can be expressed as follows:

$$\tan\alpha = 1/\omega RC \qquad (7)$$

where ω is the angular frequency, R is the resistance and C is the capacitance. A scaling law based on Equation 7 is proposed to relate the exponent r to s and t. Since C and R can both be described by a power-law equation with critical exponents s and t respectively, an addition of these two critical exponents should represent the critical exponent r for the dielectric loss tangent, $\tan\alpha$, as

$$r = t - 2s \qquad (8)$$

The factor of two associated with s in Equation 8 is the correction factor for incomplete d.c. dielectric loss of the random composite system when P is near to P_c. A comparison of the results in the Ni/F–PP system ($t = 3.1 \pm 0.3$, $s = 0.55 \pm 0.10$ and $r = 2.0 \pm 0.2$) and the Ni/N–PP system ($t = 2.1 \pm 0.1$, $s = 0.62 \pm 0.1$ and $r = 1.1 \pm 0.2$) both show good agreement with Equation 8.

A previous study [11] of a.c. response on Ag–KCl specimens shows that an equivalent circuit, as shown in the insert of Fig. 5, with a parallel combination of an ideal resistor R and a non-ideal (leaky) capacitor $C(\omega)$, can be used to describe the a.c. behaviour of random metal–insulator composite materials. Similar a.c. responses are observed in the neighbourhood of the percolation threshold of both Ni/F–PP and Ni/N–PP systems. Because the a.c. response in these two systems is so similar, only the results for Ni/F–PP will be presented. Details for both Ni/N–PP systems and the Ag–KCl system are given elsewhere [11, 14].

Fig. 5 shows the a.c. responses of a series of Ni/F–PP samples in the complex admittance plane where G is the conductance and B the susceptance. This a.c. response shown is replotted in the form of G against frequency on a log–log scale in Fig. 6. For the low Ni/F fraction samples (0.05 and 0.06), the a.c. conductivity follows a power-law dependence in frequency. For samples with a slightly higher metal concentration (0.07 and 0.08), a frequency-independent plateau of G is observed in the low-frequency range. A transition from a frequency-independent plateau to frequency-dependent power-law behaviour is

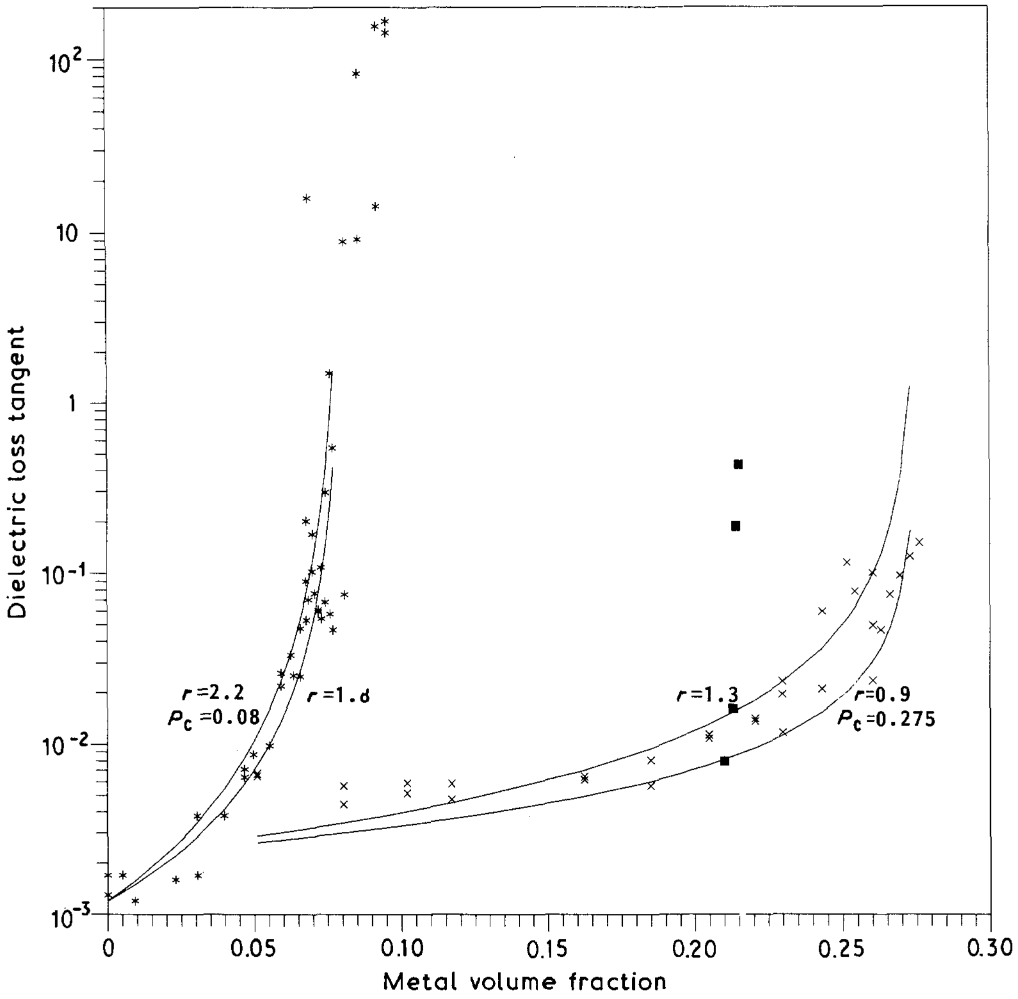

Figure 4 The dielectric loss tangent tanα as a function of metal volume fraction at 100 kHz plotted using a semi-log scale. The solid lines show Equation 6 with $P_c = 0.08$ and $r = 2.0 \pm 0.2$ for the Ni/F–PP system and with $P_c = 0.275$ and $r = 1.1 \pm 0.2$ for the Ni/N–PP system. (∗) Ni/F–PP, (×) Ni/N–PP, (■) Ag–Cl.

also observed. In these samples the transition frequency increases as the metal volume fraction increases. Further increases in the metal concentration give totally frequency-independent a.c. conductance in the frequency range studied.

The frequency dependence of the capacitance C of Ni/F–PP samples (Fig. 7) also varies with metal content. For low metal concentration (0.05), the capacitance shows nearly frequency-independent behaviour over the entire frequency range measured. With an increase in metal concentration (0.06 and 0.07), the capacitance shows an inverse frequency dependence. The degree of inverse dependence increases as the metal content increases. This effect may be accounted for by a higher a.c. conductance at higher frequency causing the release of more interface charges, and hence a decrease in the capacitance. Similar behaviour of both a.c. conductance and capacitance as a function of frequency is observed in the Ni/N–PP and Ag–KCl samples [14].

A.c. conductivity, $G(\omega)$, and a.c. dielectric constant, $K(\omega)$, of a two-dimensional thin gold film random composite near the percolation threshold have been measured in the low radio frequency range, 100 Hz to 10 MHz [29]. Similar experimental work has been performed on a three-dimensional amorphous carbon–Teflon random composite by Song *et al.* [12]. For specimens close to the percolation threshold, it is observed that both a.c. conductivity and a.c. dielectric constant follow a power-law relationship with the frequency as expressed in Equations 3 to 5, suggesting that a frequency-dependent electron–electron interaction is important as the conductive particle cluster size approaches infinity, i.e. the percolation cluster. The power-law frequency dependence of a.c. conductivity G and dielectric constant K of the random composite near the percolation threshold has been discussed by considering the polarization effects between non-contacting clusters in the composite [30] and by considering an anomalous diffusion effect within the metal cluster near the percolation threshold [31].

The exponents x and y of the three metal–insulator composites studied here have been determined by linear regression analysis and are listed in Table I, as are previously determined values. Similar a.c. conductance and dielectric behaviours are observed in all three metal–insulator composite systems, suggesting that the effects of metal morphology and insulator matrix phase do not affect the frequency-dependent electrical properties as the metal volume fraction approaches the percolation threshold. The good agreement between the values for x and y obtained here and previously [12, 29] as well as the agreement with the

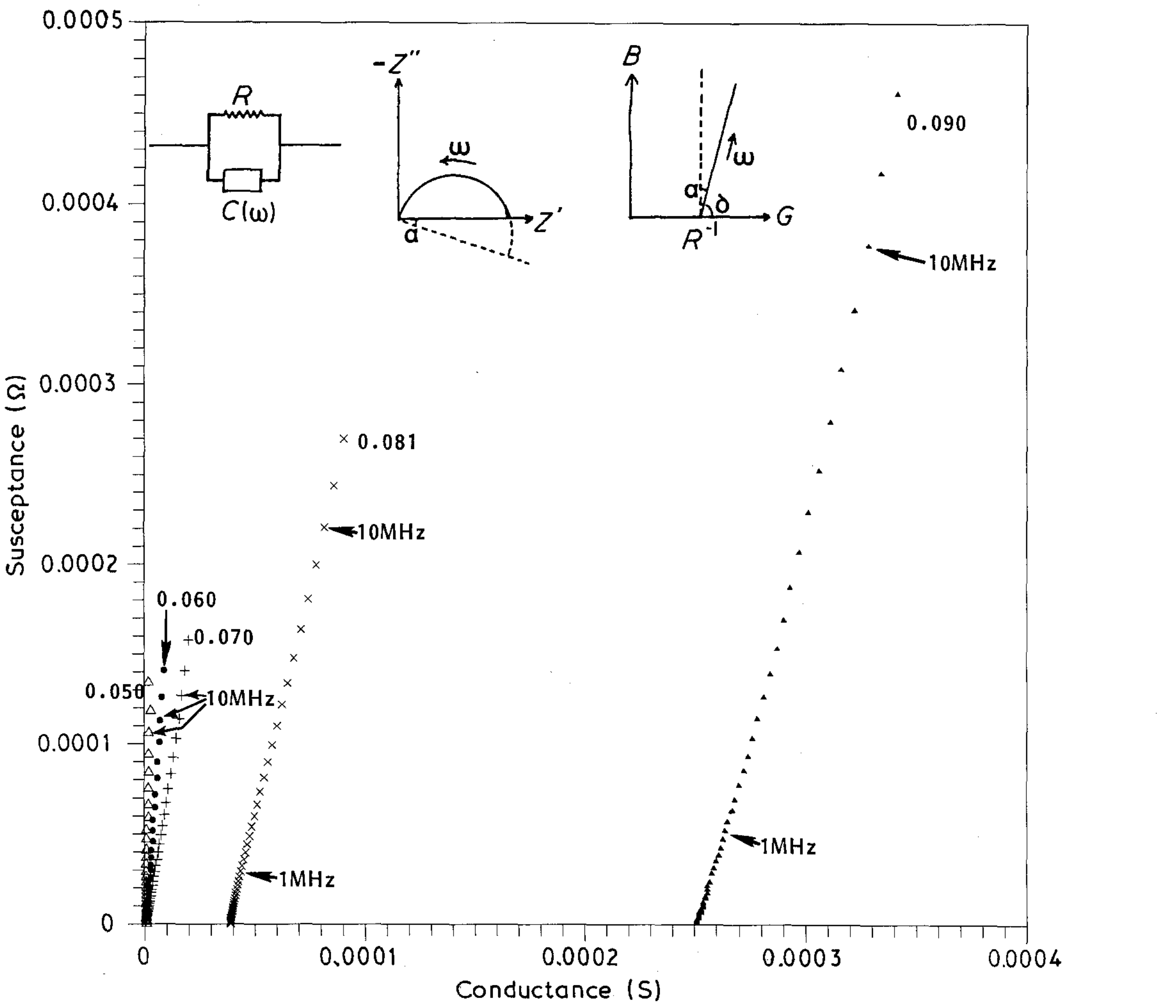

Figure 5 The a.c. response in the complex admittance plane of a series of Ni/F–PP composite samples with different Ni/F volume fractions (indicated on plots) in the frequency range from 5 Hz to 13 MHz. The inserts show the equivalent circuit with a parallel combination of resistor *R* and leaky capacitor *C* and their a.c. spectrum on a complex impedance ($-Z''$ against Z') and on a complex admittance plane (*B* against *G*).

$x + y = 1$ scaling law lend further support to this suggestion.

A wide range of dielectric materials, including polar polymers, amorphous and glassy semiconductors, and ionic conductors, show universal dielectric response in the sub-gigaHertz range [32, 33]. It has been observed [32, 33] that the a.c. conductivity $G(\omega)$ of dielectric materials shows a general frequency-dependent power law behaviour given by

$$G(\omega) \;=\; G_0 + A\omega^x \tag{10}$$

where G_0 is the frequency-independent d.c. conductivity of the specimen, A is a temperature dependent parameter, and the exponent x has a value of ~ 0.8 for various dielectric materials. A many-body interaction model has been proposed to explain this observation [32, 33]. In this model a band of correlated energy states due to the interactions between individual dipoles or charges in the nearby area allow excitations over a wide range of frequency, and thus gives rise to a frequency-dependent power-law behaviour.

Using Equation 10, which is essentially the same as Equation 3, additional insight into the conduction mechanism can be obtained. At low frequencies, the a.c. conductivity G has a frequency-independent plateau. At high frequencies, the conductivity increases as a power of frequency with the exponent x less than unity. The transition from the plateau to the power-law dependence can be explained by changing the predominant conduction mechanism from d.c. conduction through metal clusters, i.e. the G_0 term, to conduction through the insulator, which has a much lower conductivity and a frequency dependence given in Equation 10 by the ω^x term. For the special case of ionically conducting materials [34], the ionic conductivity can be extracted according to

$$G(\omega) \;=\; G_0[1 + (\omega/\omega_p)^x] \tag{11}$$

where ω_p is the ion hopping frequency associated with the dielectric loss peak.

For the metal–insulator random composite materials, the a.c. conductivity behaviour can be explained by adopting the concepts discussed above, though with a slightly different physical mechanism. At low metal volume fraction, no percolation cluster is formed and the composites behave as an insulator. The universal a.c. conduction behaviour, i.e. power-law frequency dependence, is expected in the insulator matrix. Near the percolation threshold, a percolation cluster forms and allows a limited d.c. current through these short-circuit paths. For the sample at volume

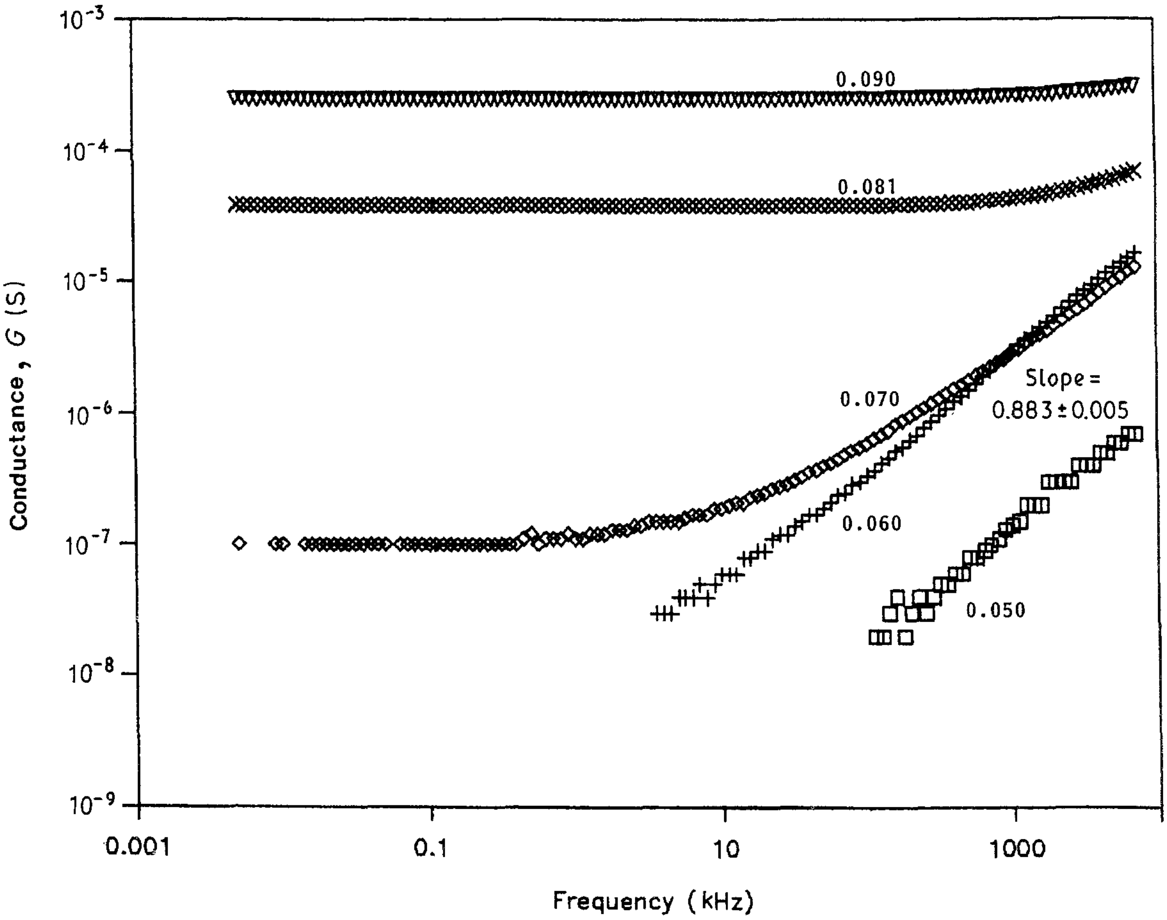

Figure 6 The a.c. conductance G as a function of frequency plotted using a log–log scale for Ni/F–PP composites. Metal volume fractions as indicated.

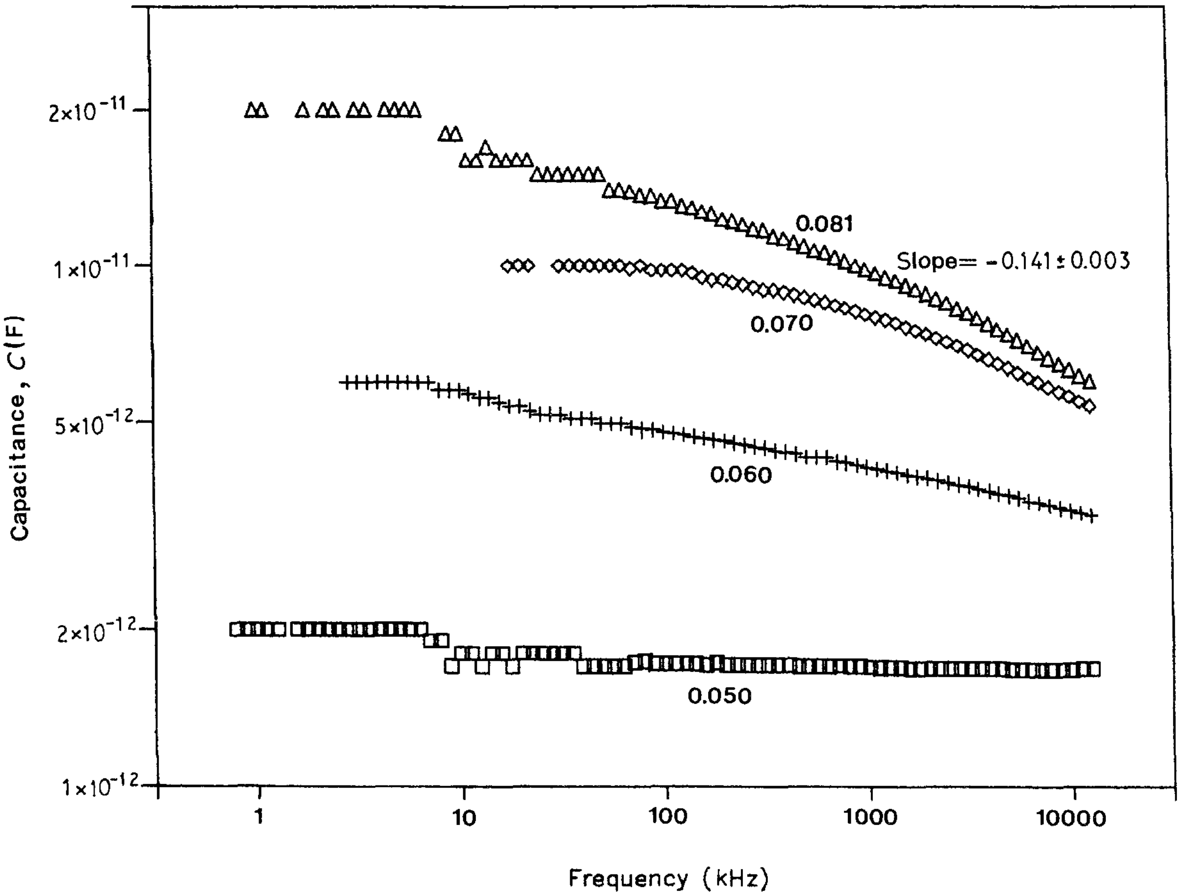

Figure 7 The capacitance C of Ni/F–PP composites as a function of frequency plotted using a log–log scale. Metal volume fractions as indicated.

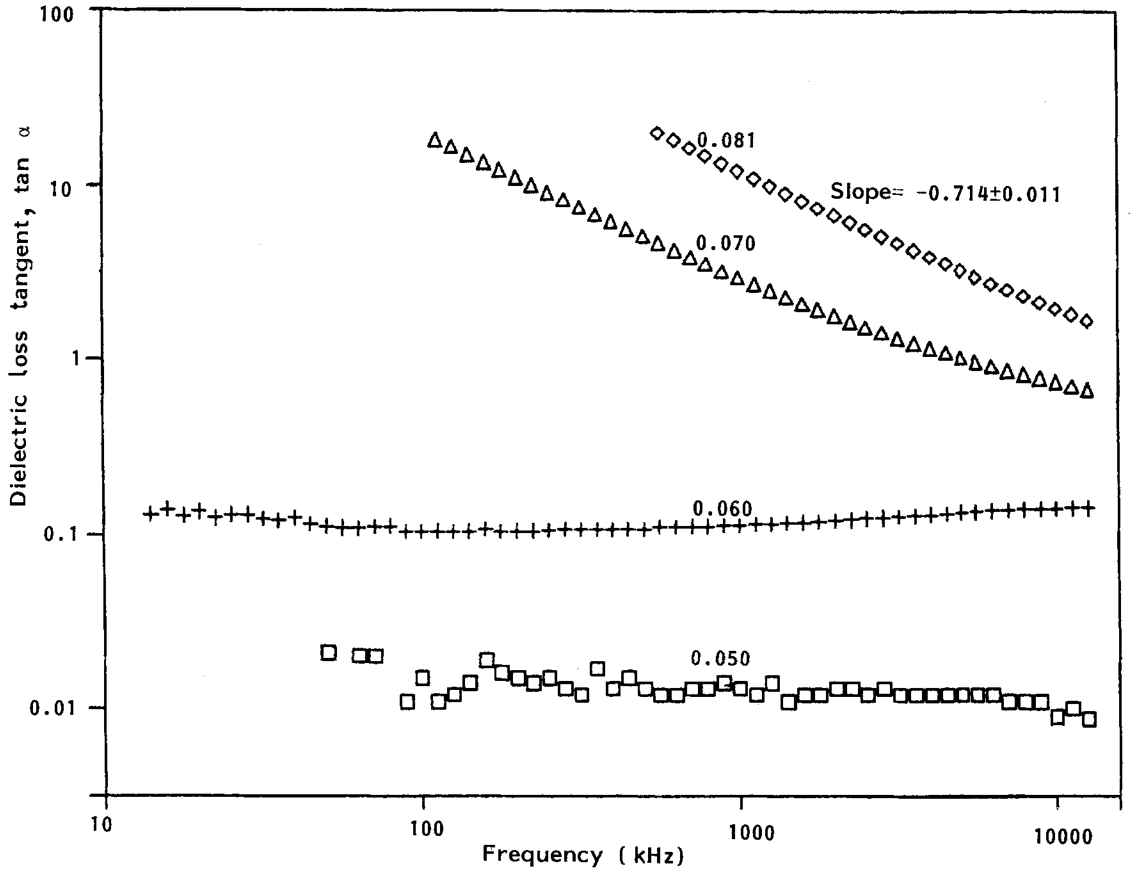

Figure 8 The dielectric loss tangent tanα as a function of frequency for Ni/F–PP samples. Metal volume fractions as indicated.

fraction equal to 0.07 in Fig. 6, transition from a d.c. conduction mechanism in the low frequency range ($\omega < 10$ kHz) to power-law behaviour in the high frequency range ($\omega > 10$ kHz) can be observed. The transition frequency continuously increases as the volume fraction (and thus the d.c. conductivity G_0) increases. Finally, only a d.c. conduction plateau will be observed for those samples with a high volume fraction and a high d.c. conductivity. It is therefore proposed that the a.c. conductivity, $G(\omega)$, is the sum of a d.c. current through metallic clusters and a.c. conduction through the insulator matrix. Equation 11 can then be applied to the metal–insulator composite, where G_0 is redefined as the conductivity of the metal clusters and ω_p is redefined as the frequency where electrical conductance by electronic conduction through the metal clusters and a.c. conduction through the insulator matrix are equivalent. Physically, ω_p may still be associated with a hopping frequency, but now it is in the presence of an electric field generated locally by the large metal clusters that exist near percolation. The value of ω_p will thus vary with metal content in the composite and is no longer a true material constant as it is in a monolithic dielectric.

The dielectric loss tangent, tanα, as a function of frequency for a series of Ni/F–PP samples near their percolation threshold is plotted in Fig. 8. For low metal volume fraction samples (such as 0.050 and 0.060), the dielectric loss tangent is essentially frequency-independent, but for high volume fraction samples (0.070 and 0.081), an inverse frequency dependence is observed. Functionally, the dielectric loss tangent can be expressed as

$$\tan\alpha \ \propto \ \omega^{-z} \tag{12}$$

where z is the critical exponent.

A gradual transition from a frequency-independent to a frequency-dependent relationship between dielectric loss tangent and applied a.c. frequency is observed. This transition can again be understood by the existence of metallic percolation clusters in the insulating matrix near the percolation threshold. The dielectric loss of the insulating material is always associated with some kind of motion of charge carriers. In the frequency range below about 1 GHz, the major process that accounts for energy dissipation is the d.c. conductivity loss which arises from both electrical and ionic charge carriers and ion hopping/dipole relaxation processes [35]. If impurity ion content is significant in the dielectric, a maximum in dielectric loss tangent will be observed at the frequency where maximum ion hopping takes place. If the dielectric loss is caused only by d.c. conductivity, the dielectric loss tangent can be expressed by Equation 7. The dielectric loss tangent will decrease monotonically as the frequency increases.

The effect of conducting paths in a matrix of dielectric material on the dielectric loss factor has been experimentally investigated by Hamon [13]. The dielectric loss factor as a function of applied frequency for a composite with segregated copper phthalocyanine powder in the matrix of paraffin wax has been studied. The dielectric loss factor was observed to spread over many decades of frequency without any clear maximum. For higher concentrations of conducting phase, the dielectric loss factor approached a straight line in accordance with the d.c. conductance loss mechanism in Equation 7. The existence of conducting paths accounts for this phenomenon.

For random metal–insulator composite samples with low metal volume fractions, no metal percolation clusters exist and the dielectric barrier between metal clusters controls the dielectric behaviour of the composite. The dielectric loss tangent is expected, then, to be frequency-independent [34] as the frequency range is far away from the ionic hopping/dipole relaxation frequency. For samples near P_c, conduction from metallic percolation clusters is important so that a frequency-dependent dielectric loss tangent should be observed. Based on the Equation 7, the loss tangent $\tan\alpha$ should follow a $1/\omega$ dependence for a pure electronic conductor, i.e. a slope of -1 in a $\tan\alpha$ against frequency log–log plot. The slope for the Ni/F–PP sample with 0.081 nickel volume fraction is measured to be -0.71 ± 0.01, which is somewhat different from -1. This may indicate that the insulator-to-metal transition of this sample is not completed.

4. Conclusions

Three systems of random metal–insulator composites, Ag–KCl, Ni/N–PP and Ni/F–PP, have been investigated near their percolation thresholds. Both dielectric constant and dielectric loss tangent diverge at the percolation threshold. The resistivity, dielectric constant and dielectric loss tangent generally follow the percolation theory prediction, i.e. a power-law dependence between electrical properties and the distance from the percolation threshold (Table I). The shape of the metal particles can have a significant effect on the critical exponents of these power-law relationships. A scaling relationship, $r = t - 2s$, is proposed to relate the exponents s and t to the loss tangent exponent, r. A relatively good agreement between the experimental results and the theory is obtained.

A simple combination of a parallel R–C circuit can be used to represent random metal–insulator composite materials with metal volume below the percolation fraction. Those composites with metal volume fractions above P_c behave as pure resistors. The studies of a.c. conductivity of dielectric materials show that for samples on the insulator side ($P < P_c$) a universal a.c. conductivity behaviour with a power-law frequency dependence is the dominant conduction mechanism in the insulating matrix. Unlike the critical exponents of conductivity, dielectric constant and dielectric loss tangent, the exponents of the frequency dependence of the conductivity and capacitance appear to be independent of the insulating matrix and the morphology of the metal particles. A transition from frequency-dependent conductivity through the insulator to frequency-independent electronic conduction through the percolating metal cluster is observed as the metal volume fraction approaches the percolation threshold. Dielectric constant and dielectric loss tangent also exhibit a transition from frequency-dependent to frequency-independent behaviour for samples near the percolation threshold. The existence of metallic percolation clusters as the metal volume fraction approaches the percolation threshold can account for these transitions.

Acknowledgements

This work, performed at the Material Research Laboratory of Ohio State University, was supported by the National Science Foundation. Special thanks are due to Drs D. Stroud, J. P. Hirth, D. A. Rigney, J. C. Garland and P. M. Hui for constructive discussions. Thanks also go to Mr B. A. Warner for providing the Ag–KCl composite specimens.

References

1. A. J. KLEIN, *Adv. Mater. Process* **1** (1986) 28.
2. S. K. BHATTACHARYA and A. C. D. CHAKLADER, *Polym.-Plast. Technol. Engng* **19** (1982) 21.
3. IN-GANN CHEN, S. SEN and D. M. STEFANESCU, *Appl. Phys. Lett.* **52** (1988) 1355.
4. F. H. STREITZ, M. Z. CIEPLAK, GANG XIAO, A. GAVRIN, A. BAKHSHAI and C. L. CHIEN, *ibid.* **52** (1988) 927.
5. S. R. BROADBENT and J. M. HAMMERSLEY, *Proc. Cambridge Philos. Soc.* **53** (1957) 629.
6. B. ABELS, H. L. PINCH and J. I. GITTLEMAN, *Phys. Rev. Lett.* **35** (1975) 247.
7. D. M. GRANNAN, J. C. GARLAND and D. B. TANNER, *ibid.* **46** (1981) 375.
8. D. STAUFFER, *Phys. Rep.* **54** (1979) 1.
9. R. ZALLEN, "The Physics of Amorphous Solids" (Wiley, New York, 1983) Ch. 4.
10. K. T. CHUNG, A. SABO and A. P. PICA, *J. Appl. Phys.* **53** (1982) 867.
11. IN-GANN CHEN and W. B. JOHNSON, *J. Mater. Sci.* **21** (1986) 3162.
12. Y. SONG, T. W. NOH, S.-I. LEE and J. R. GAINES, *Phys. Rev. B* **33** (1986) 904.
13. B. V. HAMON, *Austral. J. Phys.* **6** (1953) 305.
14. IN-GANN CHEN, PhD thesis, Ohio State University (1987).
15. H. SCHER and R. ZALLEN, *J. Chem. Phys.* **53** (1970) 3759.
16. I. BALBERG and N. BINENBAUM, *Phys. Rev. B* **35** (1987) 8749.
17. A. MALLIARIS and D. T. TURNER, *J. Appl. Phys.* **42** (1971) 614.
18. I. BALBERG and S. BOZOWSKI, *Solid State Commun.* **44** (1982) 551.
19. D. M. BIGG, *Polym. Eng. Sci.* **19** (1979) 1188.
20. I. BALBERG and N. BINENBAUM, *Phys. Rev. B* **28** (1983) 3799.
21. I. BALBERG, N. BINENBAUM and N. WAGNER, *Phys. Rev. Lett.* **52** (1984) 1465.
22. S. H. KWAN, F. G. SHIN and W. L. TSUI, *J. Mater. Sci.* **19** (1984) 4093.
23. F. F. T. de ARAUJO and H. M. ROSENBERG, *J. Phys. D: Appl. Phys.* **9** (1976) 1025.
24. A. B. HARRIS, *Phys. Rev. B.* **28** (1983) 2614.
25. D. DEPTUCK, J. P. HARRISON and P. ZAWADZKI, *Phys. Rev. Lett.* **54** (1985) 913.
26. F. CARMONA, P. PRUDHON and F. BARREAU, *Solid State Commun.* **51** (1984) 255.
27. S. KIRKPATRICK, *Rev. Mod. Phys.* **45** (1973) 574.
28. J. P. STRALEY, in "Electrical Transport and Optical Properties of Inhomogeneous Media-1977", edited by J. C. Garland and D. B. Tanner, AIP Proceedings No. 40 (American Institute of Physics, New York, 1978) pp. 118–127.

29. R. B. LAIBOWITZ and Y. GEFEN, *Phys. Rev. Lett.* **53** (1984) 380.
30. I. WEBMAN, J. JORTNER and M. H. COHEN, *Phys. Rev. B* **16** (1977) 2593.
31. Y. GEFEN, A. AHARONY and S. ALEXANDER, *Phys. Rev. Lett.* **50** (1983) 77.
32. A. K. JONSCHER, *Nature* **267** (1977) 673.
33. *Idem., J. Mater. Sci.* **16** (1981) 2037.
34. D. P. ALMOND, C. C. HUNTER and A. R. WEST, *ibid.* **19** (1984) 3236.
35. W. D. KINGERY, H. K. BOWEN and D. R. UHLMANN, "Introduction to Ceramics", 2nd Edn (Wiley, New York, 1976) p. 937.
36. C. C. CHEN and Y. C. CHEN, *Phys. Rev. Lett.* **54** (1985) 2529.

Received 21 August 1989
and accepted 19 February 1990